Momentum Resolved Radio Frequency Spectroscopy in Trapped Fermi Gases

Qijin Chen[1,2] and K. Levin[2]

[1]Zhejiang Institute of Modern Physics and Department of Physics, Zhejiang University, Hangzhou, Zhejiang 310027, China
[2]James Franck Institute and Department of Physics, University of Chicago, Chicago, Illinois 60637, USA

(Received 1 August 2008; published 15 May 2009)

We address recent momentum-resolved radio frequency (rf) spectroscopy experiments, showing how they yield more stringent tests than other comparisons with theory, associated with the ultracold Fermi gases. We demonstrate that, by providing a clear dispersion signature of pairing, they remove the ambiguity plaguing the interpretation of previous rf experiments. Our calculated spectral intensities are in semiquantitative agreement with the data. Even in the presence of a trap, the spectra are predicted to exhibit two BCS-like branches.

DOI: 10.1103/PhysRevLett.102.190402 PACS numbers: 05.30.Fk, 03.75.Hh, 03.75.Ss, 74.20.−z

Ultracold Fermi gases undergo a BCS to Bose-Einstein condensation (BEC) crossover which is tuned with a variable magnetic field. Because these atomic superfluids are viewed as quantum simulators of important condensed matter systems, (including, possibly, high T_c superconductivity [1,2]), measurements of the fermionic spectral function $A(\mathbf{k}, \omega)$ are of central importance. Recent experiments [3] on ^{40}K, near or slightly above T_c, using momentum-resolved radio frequency (rf) spectroscopy have a counterpart in angle resolved photoemission spectroscopy (ARPES) [4], and have demonstrated that these spectral functions can be directly measured. There is a substantial advantage of using ^{40}K over the more widely studied ^{6}Li since, for the usual Feshbach resonance around 202 G, there are no nearby competing resonances to introduce complications from final state interactions [5–7]. Other spectroscopic experimental tools have been proposed in the literature [8]; however, currently there are no counterpart experimental studies.

It is the purpose of this Letter to address the theoretical basis behind these measurements [3] and to show how they constrain theoretical descriptions of BCS-BEC crossover theory at finite temperatures. We also demonstrate a semiquantitative agreement with existing experiments at unitarity, and present predictions for the behavior of momentum-resolved rf spectra in a trapped gas, as one varies temperature, T, from above to below T_c. Because they elucidate the behavior of the centrally important spectral function, momentum-resolved rf experiments yield more stringent tests than other comparisons with theory provided by the ultracold Fermi gas experiments. Over the last decade [9] there has been extensive theoretical work [10–12] characterizing $A(\mathbf{k}, \omega)$ at finite T in the presence of crossover. Because of the limitations of Monte Carlo simulations at $T \neq 0$, the emphasis has been on analytical T-matrix approaches of which two different schemes have been contemplated. A comparison [10] of these approaches suggested important differences in the dispersive behavior of $A(\mathbf{k}, \omega)$.

Of the two predominant theoretical schemes, the one which we adopt [2] is shown to exhibit a robust downward dispersing (i.e., pairing) contribution in the spectral function both below and above T_c. It is also able to address the rf characteristics of a trapped superfluid gas [13,14]. The alternative scheme [11,15], which follows the approach of Nozieres and Schmitt-Rink (NSR), is somewhat less versatile. Here the downward dispersion is barely perceptible [10,16] over an extended range of $\mathbf{k}$ values, as plotted [11] for $T = 1.001T_c$. These conflicting observations need to be addressed by experiments such as in Ref. [3]. We note also that the spectral intensity maps we find evolve smoothly with temperature across T_c, also differentiating this approach from all others in the literature [17], where first order transitions are found.

There has been controversy [18] about the interpretation [6,13,14,19] of previously measured [19] spectra in unitary gases as to whether they reflect pairing or bound state [18] effects. Our calculations confirm that, by providing a clear dispersion signature in the spectral function, momentum-resolved rf spectroscopy can yield unambiguous evidence for pairing and may ultimately serve to quantify the size of the pairing gap.

In the recent rf experiments [3], pairing takes place between the 1–2 hyperfine states. An rf field of frequency ν is used to excite the atoms in hyperfine level 2 to another internal state, i.e., level 3. After the trap is turned off and the gas ballistically expands, these experiments are able to resolve the kinetic energy ϵ_k, and thereby, the three-dimensional momentum distribution of the rf-excited (or ''out-coupled'') state 3 atoms. Since the momentum of the rf photon is effectively negligible, the momenta of the out-coupled atoms are equal to that of the original 1–2 or paired states. In a homogeneous system, the contributions to the rf current from state 2 to state 3 are of two types corresponding to transitions associated with the breaking of 1–2 pairs in the condensate or with the promotion of already existing thermal fermionic excitations to level 3. In a trap the situation is similar, albeit more complex.

In the many-body theoretical derivation, it is convenient to choose the Fermi level of state 2 as zero energy. Taking Ω_L as the photon energy to excite a *free* atom in state 2 to state 3, we define Ω_L' as the level splitting between the chemical potentials for atoms in state 3 and state 2. When pairing is present, the Green's function $G(K)$ for state 2 is gapped, and the Green's function $G_3^{(0)}(K)$ for state 3 is free. We then have for the momentum-resolved rf current

$$I(\mathbf{k}, \delta\nu) = \frac{|T_k|^2}{(2\pi)^2}\int d\omega' A(\mathbf{k}, \omega' - \Omega) A_3(\mathbf{k}, \omega') \times [f(\omega) - f(\omega' + \Omega_L')] = \frac{|T_k|^2}{2\pi} A(\mathbf{k}, \omega) f(\omega)|_{\omega=\xi_\mathbf{k}-\delta\nu}, \quad (1)$$

where $A(\mathbf{k}, \omega) = -2\mathrm{Im}G(\mathbf{k}, \omega + i0)$, Ω is the rf field energy (in the absence of energy level splitting and the Fermi level mismatch between states 2 and 3), $f(x)$ the Fermi distribution function, and $T_\mathbf{k}$ the transition matrix element, which we will take to be a constant and then set to unity. This expression has been previously derived in Ref. [14], with a momentum integration. State 3 is assumed to be essentially empty $[f(\omega' + \Omega_L') = 0]$, with a free dispersion $A_3(\mathbf{k}, \omega) = 2\pi\delta(\omega - \xi_\mathbf{k} + \mu_3 - \mu)$. Note here $\delta\nu = \Omega - \mu + \mu_3 = h\nu - \Omega_L$ is the rf detuning and $\hbar = 1$. The "on-shell" condition, $\omega = \xi_\mathbf{k} - \delta\nu$, gives the energy of state 2 measured with respect to the Fermi level, where $\xi_\mathbf{k} = k^2/2m - \mu$, μ and μ_3 are the chemical potentials of atoms in state 2 and 3, respectively.

We compare this with the ARPES case where there is an "emission" process in which the photon energy is converted into the electron kinetic energy so that the electrons are knocked out of the crystal. Much like photoemission, after neglecting proportionality constants, the momentum-resolved rf experiments effectively measure [3] the "occupied spectral intensity" which corresponds to

$$I^{\mathrm{photo}}(k, \omega) \equiv \frac{k^2}{2\pi^2} A(k, \omega) f(\omega), \quad (2)$$

where the angular degrees of freedom have been integrated out. Comparing with Eq. (1), it is clear that momentum-resolved rf is essentially equivalent to ARPES. Both measure the occupied portion of the fermionic spectral function. While the strict analogy is invalidated in the presence of a trap, we will demonstrate that these momentum-resolved rf experiments are, nevertheless, capable of characterizing the spectral function of trapped gases.

Detailed numerical calculations [10] of the normal state self-energy (called Σ_{pg}) have led to a rather simple BCS-like form for the spectral function, which has been shown phenomenologically to be quite successful in applications to conventional rf [13,14] and for describing the normal phase of the cuprates [2,4,12]. Following this earlier body of work below T_c, the self-energy for a short-range two-body interaction consists of a term arising from the condensed (Σ_{sc}) as well as noncondensed pairs (Σ_{pg}). We write $\Sigma(\mathbf{k}, \omega) = \Sigma_{\mathrm{pg}}(\mathbf{k}, \omega) + \Sigma_{\mathrm{sc}}(\mathbf{k}, \omega)$, where

$$\Sigma_{\mathrm{pg}}(\mathbf{k}, \omega) = \frac{\Delta_{\mathrm{pg}}^2}{\omega + \xi_\mathbf{k} + i\gamma} - i\Sigma_0, \quad \Sigma_{\mathrm{sc}}(\mathbf{k}, \omega) = \frac{\Delta_{\mathrm{sc}}^2}{\omega + \xi_\mathbf{k}}.$$

Here the broadening $\gamma \neq 0$ and "incoherent" background contribution Σ_0 reflect the fact that noncondensed pairs do not lead to *true* off-diagonal long-range order. While we can think of γ as a phenomenological parameter in the spirit of the high T_c literature [12], there is a microscopic basis for considering this broadened BCS form [10]. The precise value of γ, and its T dependence are not particularly important for the present purposes, as long as it is nonzero at finite T. For simplicity we will take γ as a temperature independent constant throughout this Letter. Even though they both are associated with a pseudogap, we stress that the spectral function used here is rather different [10,16] from that determined by other groups which follow the NSR approach [11,15].

In Fig. 1(a), we present a contour plot of the occupied spectral intensity for the *homogeneous* case as a function of the single particle energy and wave vector k. The yellow to red regions indicate the highest intensity. The temperature here is chosen to be relatively high, around $1.9T_c$, in order to have appreciable contributions to the rf current from preexisting thermal fermionic excitations. The intensity

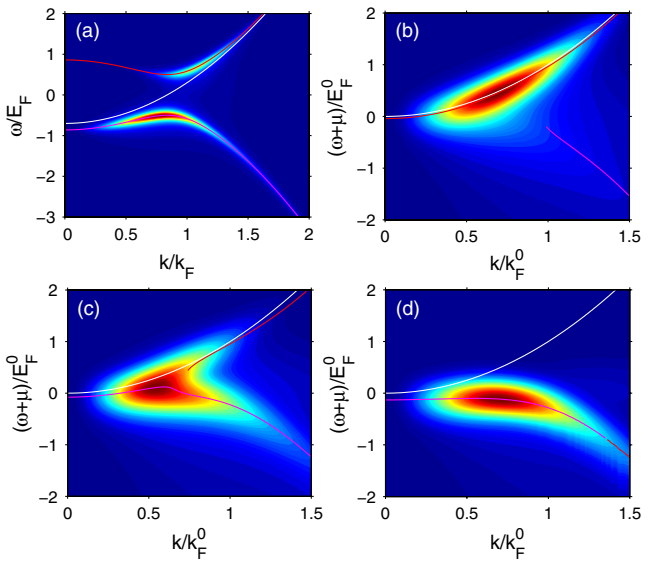

FIG. 1 (color online). Contour plots of the occupied spectral intensity $I^{\mathrm{photo}}(k, \omega)$ at unitarity (a) in the homogeneous case for $T/Tc \approx 1.9$ and in a trap for (b) $T/T_c = 1.35$, (c) 0.8, and (d) 0.1. The three lines in (a) correspond to $\pm E_\mathbf{k}$ and $\xi_\mathbf{k}$, respectively, where we take $\mu = 0.7E_F$, $\Delta = 0.5E_F$, $T = 0.4T_F$, and $\gamma = 0.1E_F$. In (b)–(d), $\Sigma_0 = 0.25E_F^0$ and $\gamma = 0.25(T/T_c)E_F^0$ at the trap center, and both scale with local density as r varies, $T_c \approx 0.27T_F^0$. The results were convoluted with a Gaussian broadening curve of width $\sigma = 0.22E_F^0$, whose value is taken from Ref. [3]. As T decreases, the spectral weight shifts from a free atom peak (upward dispersing curve) to a paired atom peak (downward dispersing curve). Here the intensity increases from dark blue for 0 to dark red for the maximum, and the lines indicate the loci of the peaks in the energy distribution curves.

map indicates upward and downward dispersing contributions, corresponding to the two rf transitions to state 3 from state 2 with dispersions $(E_{\mathbf{k}} + \mu)$ and $(-E_{\mathbf{k}} + \mu)$ relative to the bottom of the band. They reflect the broadened BCS-like form discussed above. Here, as earlier [20], Δ^2 in $E_{\mathbf{k}} = \sqrt{\xi_{\mathbf{k}}^2 + \Delta^2}$ is $\Delta^2 = \Delta_{\mathrm{sc}}^2 + \Delta_{\mathrm{pg}}^2$, with $\Delta_{\mathrm{sc}} = 0$ above T_c. The peak width in this plot comes exclusively from the incoherent terms γ and Σ_0. One can see that the bulk of the current even at this high temperature is associated with pair breaking due to the rf excitation. More generally, Fig. 1(a) describes in a conceptual way how intensity maps of this type can be used to determine the pairing gap and the presence of pairing in a less ambiguous fashion than from previous momentum-integrated experiments.

It is important to extend these calculations to include the effects of trap inhomogeneity. This is done within a local density approximation (LDA). Here it is more convenient to measure the single particle energy from the band bottom, $\omega + \mu(r) = k^2/2m - \delta\nu$, which is constant across the trap for given k. While in a homogeneous case there are two branches as described above, in a trap, a third, upward dispersing branch appears as well, corresponding to essentially free atoms at the trap edge. As is the case for the integrated rf current [13–15], this contribution dominates that of the thermally excited quasiparticles at both low and high T.

The results of the LDA-based calculations for the intensity map are shown in Figs. 1(b)–1(d) for the unitary gas in a trap, for different temperatures, calculated for typical [21] $\Sigma_0 = \gamma = 0.25E_F^0$, and convoluted with an experimental Gaussian line of width $\sigma = 0.22T_F^0$. The detailed choices for Σ_0 and γ are not essential. The vertical axis represents the single particle energy, $(\omega + \mu)/E_F^0$, where $E_F^0 = (k_F^0)^2/2m$ is the global Fermi energy in the noninteracting limit. The temperatures are (b) $T/T_c = 1.35$ (above T_c), (c) 0.8 (slightly below T_c), and (d) 0.1 (well below T_c). At the highest T the central notable feature is a single upward dispersing curve which fits the free particle dispersion; here the spectral weight is dominated by contributions from atoms at the trap edge. This dispersion can be readily differentiated from that associated with preexisting thermally broken pairs which varies as $E_{\mathbf{k}} + \mu$ and, of course, depends on the distribution of energy gaps $\Delta(r)$.

As T decreases a second (downward dispersing) branch becomes evident, which is associated with the breaking of a condensed pair and necessarily contains trap-averaging effects. The intensity map first bifurcates and eventually at very low T becomes dominated by the lower branch, when essentially all atoms are paired. Just as in the homogeneous case discussed in Fig. 1(a), a BCS-like fit to this dispersion can be used to determine the pairing gap.

In Fig. 2(a) we plot the energy distribution curves (EDC) for a series of momenta k in a unitary trapped Fermi gas at $T/T_c = 1.1$. Here we have taken a somewhat larger intrinsic and instrumental broadening than in Fig. 1. These parameters are seen to optimize semiquantitative agreement with the data. These EDCs can be compared with their counterparts plotted in Fig. 4 in Ref. [3]. At small k there is a single peak which separates into two at higher k. The data are not sufficiently smooth to be assured that two peaks are visible at larger k, but they are consistent with this picture [22]. As before, we attribute the separation at higher k to the fact that the upward and downward dispersing curves become most well separated in this regime. Better agreement is expected with improved signal-to-noise ratio in the data. Moreover, including detailed incoherent background contributions in the fermionic self-energy may also improve the agreement with experiment.

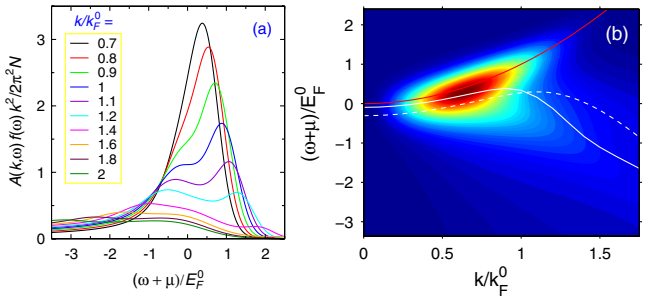

FIG. 2 (color online). (a) Energy distribution curves for a series of momenta k and (b) corresponding occupied spectral intensity map, in a unitary trapped Fermi gas at $T/T_c = 1.1$. Here $\Sigma_0 = 0.35E_F^0$ and $\gamma = 0.38E_F^0$ at the trap center, and $\sigma = 0.3E_F^0$. In (b), the red curves represent the free atom dispersion, while the white solid and dashed curves are the quasiparticle dispersion obtained theoretically and experimentally [3], respectively, via fitting the EDCs with a single Gaussian distribution.

Figure 2(b) presents the corresponding spectral intensity map. The white dashed curve represents a fit of the experimental peak dispersion [3] while the solid white curve is the theoretical counterpart. Here, following experiment we have fit the EDC to a *single* Gaussian peak. The comparison between the two white curves shows semiquantitative consistency. Moreover, both can be well fit to the BCS dispersion involving $E_{\mathbf{k}}$, as was originally proposed in Ref. [10]. Indeed Fig. 2(b) seems to capture the essential results shown in Fig. 3(a) in Ref. [3]. The fact that the experiments were done near T_c suggests that there is a sizable pseudogap at and above T_c at unitarity.

We finally show in Fig. 3(a) the intensity map on the BEC side of resonance for $1/k_F^0 a = 1.1$ at $T/T_c = 1.3$, where $T_c \approx 0.3T_F^0$, and a is the s-wave scattering length. Even at this relatively high temperature there is virtually no weight in the free atom peak, associated with atoms at the trap edge. All the atoms are bound into pairs and there is only one downward dispersing peak in the plot. This behavior can be contrasted with that shown in Fig. (3c) of Ref. [3] where there is a free atom contribution, which has been attributed to unpaired atoms out of chemical equilibrium with the pairs. In addition, the peak in Fig. 3(a) is rather sharp. In contrast, the large peak width in Ref. [3] seems to suggest incoherent contributions to the fermionic self-energy, which may have to do with chemical nonequi-

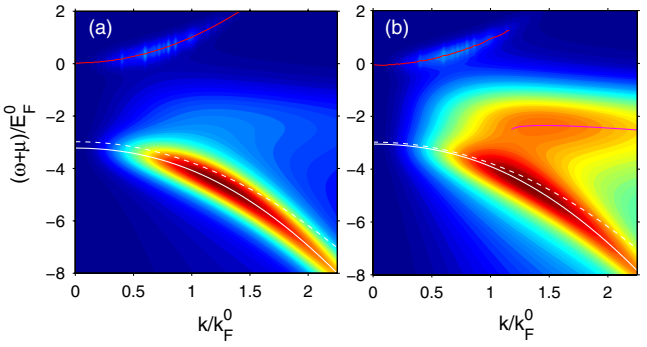

FIG. 3 (color online). Occupied spectral intensity maps $I^{\text{photo}}(k, \omega)$ at $1/k_F^0 a = 1.1$ in the BEC case and $T/T_c = 1.3$. The broadening parameters at the trap center are (a) $\Sigma_0 = 0.35E_F^0$ and $\gamma = 0.45E_F^0$ and (b) $\Sigma_0 = 1.0E_F^0$ and $\gamma = 1.3E_F^0$. For both, $\sigma = 0.25E_F^0$. Coherent sharp quasiparticle peaks can be seen in (a). Larger broadening in (b) makes the coherent peak less pronounced, mimicking possible effects of chemical nonequilibrium. The red curve represents free atom dispersion, and the solid and dashed white curves represent the theoretical and experimental quasiparticle dispersion, respectively.

librium. The underlying theory here presumes that there are still well-defined quasiparticles on the BEC side of resonance. We present in Fig. 3(b) the case in which we have considered a substantially larger intrinsic broadening $\gamma \approx \Delta$ to represent some of the qualitative features of the experimental data.

In conclusion, we have shown how momentum-resolved rf spectroscopy can be used to measure the centrally important spectral function of ultracold Fermi gases. Unique to the present experiments is the fact that one can use the related dispersive behavior to distinguish the various trap contributions, say preexisting thermally broken pairs from trap edge effects. Thus, because they establish the actual dispersion associated with the rf current contributions, these experiments can remove theoretical and experimental ambiguities. Moreover, they are able to weigh in on the different analytical approaches to BCS-BEC crossover [2,10,11]. The two predominant schemes differ in whether, as in NSR, there are two bare Green's functions in the T-matrix series or as here, one dressed and one bare Green's function which is known [23] to be associated with the structure of BCS theory. This second approach leads to a stronger pseudogap, since there is already a gap in the T-matrix which, in turn, stabilizes longer lived pairs. Not surprisingly, only for this scheme does $A(\mathbf{k}, \omega)$ exhibit more than a barely perceptible [10,11,16] downward dispersion of the BCS form.

Because both approaches yield two peaks in the spectral function, the absence of a BCS-like dispersion in the alternative approach shows that the "pseudogap" state is different in the two theories. In a related fashion, there is a contribution to the rf current, associated with a negative detuning peak [7] which corresponds to thermal quasiparticles with dispersion $-E_{\mathbf{k}}$. However, only one peak is obtained in the weaker pseudogap scheme [15] within the normal (homogeneous) phase. We believe that both theoretical approaches are relevant, but over different temperature regimes, and that it is plausible that the BCS-like correlations and stronger pseudogap which are found here quite naturally evolve at even higher T into this weaker pseudogap phase which has been widely studied [11,15]. More work will be needed to address this issue but it does point to a very interesting normal state.

This work is supported by NSF PHY-0555325 and NSF-MRSEC Grant No. DMR-0213745 and by Zhejiang University. We thank D. S. Jin, J. T. Stewart, J. P. Gaebler, and E. Mueller for many useful communications.

[1] A. J. Leggett, Nature Phys. **2**, 134 (2006).
[2] Q. J. Chen, J. Stajic, S. N. Tan, and K. Levin, Phys. Rep. **412**, 1 (2005).
[3] J. T. Stewart, J. P. Gaebler, and D. S. Jin, Nature (London) **454**, 744 (2008).
[4] A. Kanigel *et al.*, Phys. Rev. Lett. **101**, 137002 (2008).
[5] A. Perali, P. Pieri, and G. C. Strinati, Phys. Rev. Lett. **100**, 010402 (2008); M. Punk and W. Zwerger, *ibid.* **99**, 170404 (2007); Z. Yu and G. Baym, Phys. Rev. A **73**, 063601 (2006).
[6] S. Basu and E. Mueller, Phys. Rev. Lett. **101**, 060405 (2008).
[7] Y. He, C. C. Chien, Q. J. Chen, and K. Levin, Phys. Rev. Lett. **102**, 020402 (2009).
[8] T. L. Dao, A. Georges, J. Dalibard, C. Salomon, and I. Carusotto, Phys. Rev. Lett. **98**, 240402 (2007).
[9] B. Jankó, J. Maly, and K. Levin, Phys. Rev. B **56**, R11 407 (1997).
[10] J. Maly, B. Jankó, and K. Levin, Physica (Amsterdam) **321C**, 113 (1999); Phys. Rev. B **59**, 1354 (1999).
[11] A. Perali, P. Pieri, G. C. Strinati, and C. Castellani, Phys. Rev. B **66**, 024510 (2002).
[12] Q. J. Chen and K. Levin, Phys. Rev. B **78**, 020513(R) (2008).
[13] J. Kinnunen, M. Rodriguez, and P. Törmä, Science **305**, 1131 (2004); Phys. Rev. Lett. **92**, 230403 (2004).
[14] Y. He, Q. J. Chen, and K. Levin, Phys. Rev. A **72**, 011602 (R) (2005).
[15] P. Massignan, G. M. Bruun, and H. T. C. Stoof, Phys. Rev. A **77**, 031601(R) (2008).
[16] E. Mueller (private communication).
[17] P. Pieri, L. Pisani, and G. C. Strinati, Phys. Rev. B **70**, 094508 (2004); R. Haussmann, W. Rantner, S. Cerrito, and W. Zwerger, Phys. Rev. A **75**, 023610 (2007); N. Fukushima, Y. Ohashi, E. Taylor, and A. Griffin, *ibid.* **75**, 033609 (2007); H. Hu, P. D. Drummond, and X. J. Liu, Nature Phys. **3**, 469 (2007).
[18] C. H. Schunck, Y. Shin, A. Schirotzek, M. W. Zwierlein, and W. Ketterle, Nature (London) **454**, 739 (2008).
[19] C. Chin *et al.*, Science **305**, 1128 (2004).
[20] Q. J. Chen, I. Kosztin, B. Jankó, and K. Levin, Phys. Rev. Lett. **81**, 4708 (1998).
[21] Q. J. Chen, K. Levin, and I. Kosztin, Phys. Rev. B **63**, 184519 (2001).
[22] D. S. Jin (private communications).
[23] L. P. Kadanoff and P. C. Martin, Phys. Rev. **124**, 670 (1961).